

Potential interplay between AQP1 and Cltx, and pharmacological antagonism of glioblastoma-enriched membrane proteins reduce glioblastoma cell motility

A thesis submitted in partial fulfillment of the

HONOURS DEGREE of BACHELOR OF

HEALTH AND MEDICAL SCIENCES In

The Discipline of Physiology
Adelaide Medical School

The University of Adelaide

by Alanah Varricchio

June 2020

Abstract

The highly invasive nature of glioblastoma makes it difficult to treat with strategies aimed at eliminating primary tumours. Discovery of pharmacological inhibitors that restrict tumour motility could improve clinical outcomes. Chlorotoxin (Cltx), isolated from *Leiurus quinquestriatus* venom, limits glioblastoma tumour cell motility albeit via elusive mechanisms. I hypothesised that aquaporin-1 (AQP1), a dual water and cation channel upregulated in glioblastoma, could be an unrecognised target of Cltx given its documented roles in facilitating cellular motility pathways. Transcriptomic database analyses identified membrane proteins in addition to AQP1 with elevated transcript levels in human glioblastoma biopsies and implications in pathways facilitative of tumour growth, including glutamate receptors, and Ca²⁺ and K⁺ channels. I hypothesised that selective antagonists of these membrane proteins would decrease glioblastoma cell invasion. Cell motility was measured with invasion and wound closure assays in cultured glioblastoma cells. Swelling assays and two-electrode voltage clamp assessed AQP1 channel function in AQP1-expressing oocytes. Studies investigated two aims: the proposed Cltx-mediated block of AQP1 ion channels and the invasion-limiting effects of selective inhibitors of ligand- and voltage-gated ion channels in glioblastoma cell lines. Results showed that Cltx impaired glioblastoma cell invasion by approximately 25% ($p < 0.01$) but did not affect cell migration or AQP1 water or ion channel activities, discounting AQP1 as a target of Cltx action. Antagonists of AMPA/kainate, Ca²⁺ and K⁺ channels inhibited cellular invasion by $\geq 25\%$ ($p < 0.001$) at non-cytotoxic concentrations, suggesting promise as adjunct therapies to limit glioblastoma cell motility during administration of primary treatments.

Words: 249

Introduction

Glioblastoma (also known as glioblastoma multiforme; GBM) is a highly malignant grade IV glioma that represents 15 to 20% of all intracranial tumours.¹ Current treatment strategies combine surgical resection, radiation and chemotherapy; however, diffuse infiltration of glioma cells into healthy brain parenchyma makes successful interventions nearly impossible. Glioma often gain adaptive resistance via genetic changes following recurrent chemotherapy,² imposing poor prospects for patient survival. Despite advances in surgery, radiotherapy and chemotherapy, the median survival expectancy of glioblastoma patients after

diagnosis is only 12 to 14 months.³

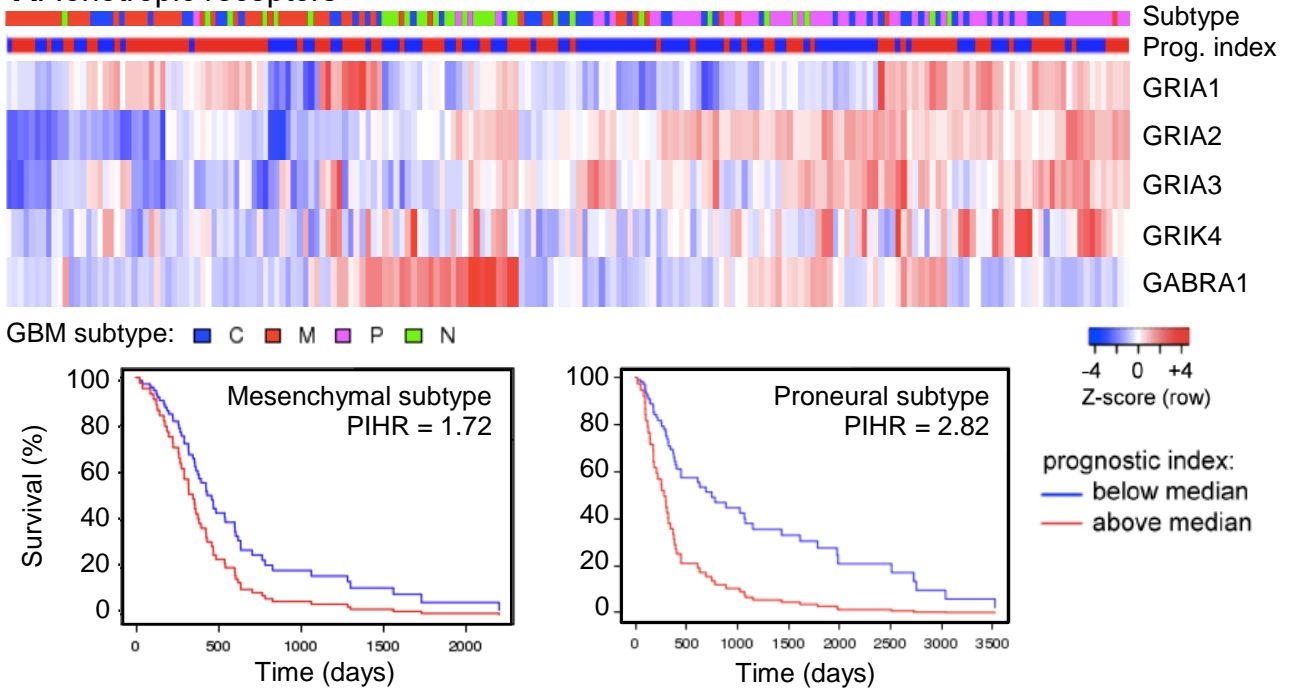
Innovative therapeutic development is needed for clinically challenging diseases such as glioblastoma. An ideal candidate drug should elicit the desired physiological effects via selective and specific interactions with its protein targets in a complex molecular background to maximise efficacy and limit adverse side-effects.⁴ Evoking desired effects at low concentrations is a favourable characteristic, provided high potency is without increased side-effects.⁵ Accessibility to the target via the route of therapeutic administration and a suitable response time following interaction are also critical factors.⁵

A systematic correlation of phenotypes with molecular markers has identified diagnostic indicators of three major subtypes of GBM: proneural, classical and mesenchymal with the existence of a fourth, neural subtype remaining under question.⁶ The Human Protein Atlas (TCGA) database provides quantitative transcriptomic data from human glioblastoma biopsy samples, allowing identification of genes with altered expression levels (quantified as FPKM; fragments per kilobase of transcript per million fragments mapped). The GBM Bio Discovery portal supports user-specified interrogation of the TCGA database to define sets of glioblastoma-enriched genes and evaluate their prognostic index hazard ratio (PIHR), with larger ratios indicating poorer prognosis. Classes of ionotropic receptors, water channels and voltage-gated ion channels upregulated in glioblastoma (**Table 1** and **Figure 1**) could serve as novel candidate targets for glioblastoma interventions.

Table 1: Ionotropic receptors, water channels and voltage-gated ion channels with enriched transcript levels in human glioblastoma biopsy samples ($n = 153$) and percent survival at 3 years for patients with FPKM > median analysed using TCGA RNAseq (Human Protein Atlas database); PIHR analysed with GBM Bio Discovery Portal. Adapted from Yool and Ramesh.⁷

Gene	Classification	PIHR	Median FPKM	% survival
Ionotropic receptors				
GRIA1	AMPA receptor	1.12	7.5	7
GRIA2	AMPA receptor	1.03	5.6	11
GRIA3	AMPA receptor	0.96	8.5	10
GRIK4	Kainate receptor	0.74	3.0	13
GABRA1	GABA _A receptor	1.01	0.3	12
Water and voltage-gated ion channels				
AQP1	Aquaporin-1	1.06	240	12
CLCN3	Cl ⁻ channel	0.90	19	13
CACNA1A	Ca ²⁺ channel	0.99	1.2	6
CACNA1G	Ca ²⁺ channel	1.08	0.97	6
KCNA2	K ⁺ channel	1.12	1.0	14
KCND2	K ⁺ channel	1.02	4.3	12

A: Ionotropic receptors



B: Water and ion channels

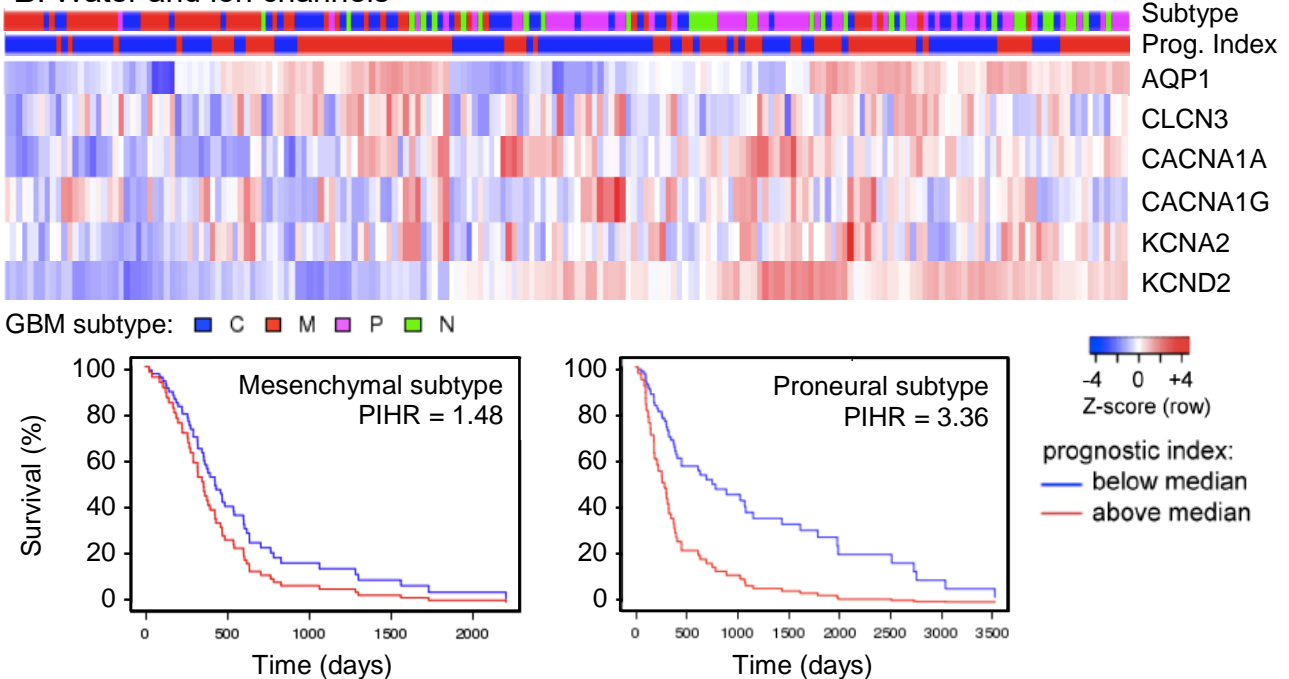


Figure 1: Evaluation of expression patterns for the classes of (A) ionotropic receptors and (B) water and ion channels presented in **Table 1**. Data were analysed using the GBM Bio Discovery Portal and are presented in heat maps (above) summarising transcript expression (FPKM, colour bars) in GBM subtypes and Kaplan Meier survival curves (below) for mesenchymal and proneural subtypes. Heat map columns represent individual GBM patient data and show transcript levels for each gene in the class as a Z-score relative to the average transcript level across the sample population, with predominantly low (blue) and high (red) expression on the left and right respectively. GBM subtypes⁶ are assigned to patients (topmost row) as per the colour key.

Aquaporin-1 (AQP1)

Aquaporins are integral membrane proteins with fundamental roles in transporting water across biological membranes and regulating cellular volume.⁸ AQP1, one of fifteen mammalian aquaporins identified to date,⁹ is permeable to water and monovalent cations K^+ , Cs^+ , Na^+ and Li^+ .^{10,11} AQP1 is primarily expressed in cell types involved in water transport, including renal tubules and the choroid plexus,¹² with amplified transcript levels observed in glioblastoma tumours (**Table 1**). AQP1 is implicated in migration and invasion events underpinning cell dispersal.^{13,14} AQP1 gene silencing reportedly decreased migration and invasion in glioma-derived cell lines, and impaired tumourigenesis *in vivo* after xenographic implantation of shRNA-AQP1-transfected human glioma cells into nude mice.¹³ Passage of glioma cells through narrow extracellular spaces in the brain is thought to be enabled by cell shrinkage following efflux of Cl^- , K^+ and water.¹⁴ K^+ efflux occurs in part via AQP1, based on observations of potent block of glioma cell invasion by AQP1 ion channel blocker AqB011.¹⁵

Voltage-gated chloride channels (CICs)

CICs are ubiquitously expressed in all cells and are fundamental to osmoregulation. Cl^- channel CIC-3, with increased transcript levels in glioblastoma (**Table 1**), is thought to facilitate Cl^- efflux, enabling glioma cell shrinkage¹⁴ and facilitating cell movement through brain tissue.

Chlorotoxin (Cltx) is a 36-residue peptide isolated as a putative Cl^- channel antagonist from *Leiurus quinquestriatus* venom.¹⁶ Cltx interferes with protein trafficking by binding a cell-surface macromolecular complex containing extracellular matrix-degrading metalloproteinase-2 and co-localised CIC-3, inducing internalisation and consequently disrupting glioblastoma invasion.¹⁷ Interaction between Cltx and annexin A2 is also documented, with siRNA knockdown of annexin A2 preventing Cltx derivative TM-601 from binding to glioma tumour cells.¹⁸ With multiple Cltx binding partners proposed,^{17,18} elucidating the mechanism(s) by which Cltx disrupts glioblastoma progression has proven challenging and suggests that additional targets of Cltx remain to be discovered.

Cltx is positively charged at physiological pH¹⁶ and could show affinity for AQP1 cation channels. Given the established roles of AQP1 and CIC-3 ion channels in facilitating glioma cell motility,^{13,19} it is reasonable to

surmise an interaction between AQP1 ion channels and Cltx that suppresses invasion and migration of glioblastoma.

Non-NMDA glutamate receptors

Ionotropic glutamate receptors dispersed throughout the mammalian central nervous system are essential for generating postsynaptic neuron excitation by modulating ion channels.²⁰ Receptors are categorised primarily by pharmacological agonist sensitivities into NMDA (N-methyl-D-aspartate) and non-NMDA subtypes. Non-NMDA receptors are activated by AMPA (alpha-amino-3-hydroxy-5-methyl-4-isoxazolepropionic acid (AMPA), and kainate.²¹

Analysis of ligand-gated ion channels in glioblastoma showed that non-NMDA receptors had the highest transcript levels, contrasting with comparatively low levels for GABA_A receptors (**Table 1**). Ca²⁺ signalling via AMPA-type receptors was suggested to promote growth and motility of glioblastoma cells via activation of Akt, a protein kinase central to many anabolic pathways.²² Overexpression and activation of Ca²⁺-permeable AMPA receptors in glioblastoma increased migration and proliferation whilst loss of AMPA-mediated Ca²⁺ permeability curtailed glioblastoma cell locomotion and induced apoptosis.²³

Voltage-gated calcium (Ca_v) channels

Ca_v channels are expressed in most cells and serve distinct roles in signal transduction. In response to depolarised membrane potentials, Ca_v channels open and mediate influx of Ca²⁺, a second messenger that initiates many physiological events.²⁴ Two general categories of Ca_v channels are defined by biophysical properties: (1) high voltage-activated that open in response to strong membrane depolarisation and (2) low voltage-activated that open upon weak depolarisation.²⁵ Ca_v channel transcript levels are notably increased in glioblastoma (**Table 1**). Ca_v3-dependent Ca²⁺ influx has proven important to glioblastoma disease progression, with significantly decreased glioblastoma proliferation observed *in vitro* following inhibition of Ca_v3 channels with antisense oligonucleotides or non-selective antagonist mibefradil.²⁶

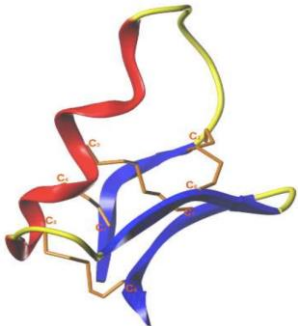
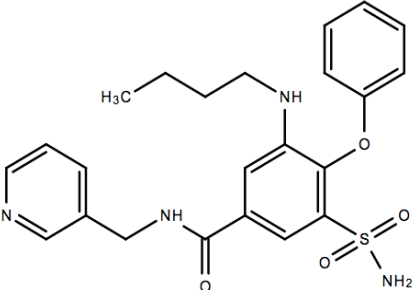
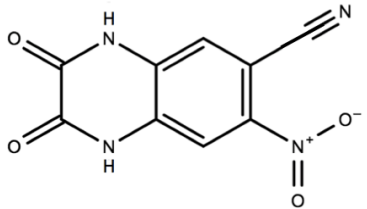
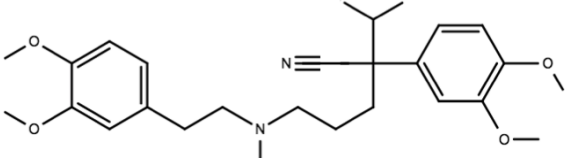
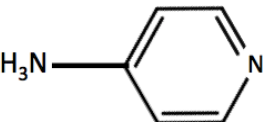
Voltage-gated potassium (K_v) channels

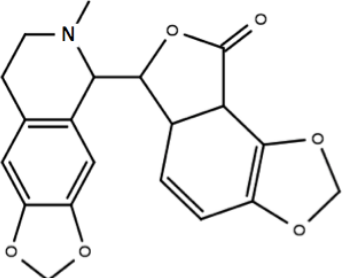
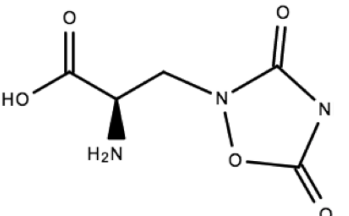
K_v channels, the largest group of human channel proteins, are widely distributed throughout the nervous system and other tissues,²⁷ with particularly elevated expression in glioblastoma (**Table 1**). K_v channels are best known for regulating neuronal firing patterns by facilitating K⁺ efflux after membrane depolarisation to rapidly repolarise the membrane and create the falling phase of action potentials.²⁸ More broadly, K_v channels participate in signalling pathways underlying cellular proliferation to allow progression of the cell cycle past the G₁ checkpoint.²⁹ In oligodendrocyte precursors, K_v channel inhibition induces cell cycle arrest at G₁ following accumulation of p27 and p21 cyclin-dependent kinase inhibitors.³⁰

The aforementioned studies characterising the significance of perturbing AMPA/kainate, Ca_v and K_v channels in glioblastoma are within the vast majority of cancer drug discovery endeavours whose primary outcomes of interest are apoptosis and reducing proliferation.^{23,26,29,30} Contrarily, therapeutic methods for managing cancer cell metastasis, a major cause of cancer-related deaths, are scarce. Dexamethasone, a synthetic glucocorticoid used to treat glioblastoma-induced brain oedema, reportedly inhibits glioblastoma migration by reducing metalloproteinase-2 secretion³¹ and perturbing the MAPK/ERK pathway.³² However, these ideas remain controversial following starkly contrasting accounts of dexamethasone increasing glioma cell migration by upregulating AQP1 expression.³³ A novel concept tested here was that pharmacologically antagonising glioblastoma-enriched ion channels should impair glioblastoma motility pathways. Modulating glioblastoma diffusion using this approach would constitute a powerful adjunct therapy when applied in parallel with existing procedures aimed at direct eradication of primary tumours.

This project initially focused on determining the effects of Cltx on the (1) percentage of invasion and migration in AQP1-enriched glioblastoma cell lines and (2) swelling rate (in hypotonic saline) and ionic conductance of AQP1-expressing *Xenopus laevis* oocytes. I hypothesised that prolonged Cltx exposure would decrease (1) motility of cultured glioblastoma cells and (2) ionic conductance via AQP1 ion channels in oocytes. A broader search for potent *in vitro* inhibition of glioblastoma invasion was then conducted using agents targeting glioblastoma-enriched ligand- and voltage-gated ion channels. Antagonistic agents were expected to potently decrease invasiveness of cultured glioblastoma cells given the roles of their protein targets in cellular motility pathways.

Table 2: Properties of selected compounds reported to affect glioblastoma-enriched ion channels *in vitro*

Name	Chemical/Molecular Structure	Known Target(s)	Effect(s)
Cltx		CIC-3, metalloproteinase-2, annexin A2	Inhibits protein trafficking ¹⁷ and annexin A2-mediated cellular migration ¹⁸
AqB011		AQP1	Cation transport antagonist ¹⁵
Cyanquixaline		AMPA/kainate receptors	Blocks responses to Ca ²⁺ , AMPA and kainate ³⁴
Verapamil		Cav channels	Ca ²⁺ transport antagonist ³⁵
4-aminopyridine		K _V channels	K ⁺ transport antagonist ³⁶

Bicuculline	 <p>The chemical structure of Bicuculline consists of a piperidine ring with a methyl group on the nitrogen atom, connected to a benzene ring. This benzene ring is further connected to a bicyclic system containing a five-membered ring with an oxygen atom and a carbonyl group, and a six-membered ring with an oxygen atom.</p>	GABA _A receptors	Cl ⁻ transport antagonist ³⁷
Quisqualic acid	 <p>The chemical structure of Quisqualic acid features a central carbon atom bonded to a hydroxyl group (HO-), an amino group (H₂N) shown with a wedge bond, and a propyl chain. The terminal carbon of the propyl chain is attached to a five-membered ring containing two nitrogen atoms and two carbonyl groups.</p>	AMPA/kainate glutamate receptors	Cation transport agonist ³⁸

Materials & Methods

Cell lines

Human glioblastoma cell lines U-87MG and U-251MG were purchased from American Type Culture Collection (ATCC, Manassas, VA) and cultured in Dulbecco Modified Eagle Medium (DMEM, Gibco) containing 10% foetal bovine serum (FBS, Life Technologies), 1% GlutaMAX (Gibco) and 100 units/mL each of penicillin and streptomycin (Life Technologies). Cell cultures were grown at 37°C in a humidified 5% CO₂ incubator.

Transwell Invasion Assay

Invasion assays were performed as previously described³⁹ in 24-well transwell inserts (6.5 mm, 8 µM pores; Corning® Transwell polycarbonate; Sigma-Aldrich) layered with extracellular matrix gel (Matrigel; Sigma-Aldrich). Briefly, cultures were grown to 40% confluency before starvation in DMEM containing 2% FBS. After 24 h, cells were detached (with 1% trypsin and 0.5% EDTA in PBS) and resuspended in FBS-free DMEM. Cells were seeded in transwell inserts totalling 150 µL of cell suspension (5 x 10⁴ cells/mL) per well, including 50 µL of FBS-free rehydration medium. Compounds of interest or 0.1% dimethylsulfoxide (DMSO; vehicle control) were added at appropriate concentrations. Compound concentrations were chosen based on results reported in the literature cited in **Table 2** and with regard to solubility limits and ideal solvent information provided by suppliers; Sigma-Aldrich or in the case of Cltx, A/Prof. Mehdi Mobli (Centre for Advanced Imaging, The University of Queensland). Chemoattractant gradients were created with DMEM (10% FBS) containing the relevant compound of interest or control treatment. Following 4 h incubation, non-invasive cells were removed from upper surfaces of filters. Invasive cells on bottom surfaces were stained with crystal violet (0.2% w/v, Sigma-Aldrich) and live-imaged with EOS Utility 3 (Canon, USA) on an inverted microscope (ULWCD 0.30, Olympus Corp., Tokyo, Japan.). Percentage of invasion under each condition was calculated from the average number of invasive cells per well across three randomly selected fields (20x objective) appropriately standardised to the overall vehicle or untreated control mean. Independent experiments were repeated twice, with up to four replicates.

Wound Closure Assay

Cells were grown to 40% confluency in 96-well plates before starvation in DMEM (2% FBS) containing

mitotic inhibitor 5-fluoro-2-deoxyuridine (FUdR; 100 ng/mL) for 24 h. Confluent monolayers were wounded by aspirating ~80 μm^2 with a 200 μL pipette tip. Medium was replaced with DMEM (2% FBS, 100 ng/mL FUdR) containing drug-based or vehicle control (0.1% DMSO) treatments. Wound areas were imaged at 0 and 24 h (10x objective; Canon EOS 6D, Canon, Tokyo, Japan) on an inverted microscope (ULWCD 0.30, Olympus Corp., Tokyo, Japan). ImageJ software (U.S. National Institutes of Health (NIH), MD, USA) quantified wound closure resulting from cellular migration as the percentage of cell-occluded area at 24 h. Experiments were independently repeated twice, with six to eight replicates.

Cytotoxicity Assay

Cell viability was measured with the Alamar Blue assay⁴⁰ according to the manufacturer's instructions (Thermo Fisher Scientific). Cells were seeded in 96-well plates in DMEM (10% FBS). Following overnight incubation, drug-based and vehicle control treatments were applied and cultures were incubated for 4 h. After 90 min incubation with 10% Alamar Blue in DMEM (10% FBS), fluorescence was measured using FLUOstar Optima microplate reader. A control sample with DMEM only (no cells) was included for background colour subtraction.

Osmotic Swelling Assays

Oocytes were harvested from anaesthetised *Xenopus laevis* frogs in accordance with the Australian Code of Practice for the Care and Use of Animals for Scientific Purposes. Wild-type AQP1-expressing oocytes were prepared as per previous methods.⁴¹ For double-swelling assays, each oocyte was its own control, with swelling rates in Cltx-free 50% hypotonic Na^+ saline (isotonic Na^+ saline diluted into an equal volume of water) measured first (S1). The second assay (S2) measured swelling rates following 20 min incubation in isotonic saline \pm Cltx (1 μM). Swelling rates were quantified by relative increases in oocyte cross-sectional area following greyscale imaging with a camera (Cohu, San Diego, CA) mounted on a dissecting microscope (Olympus SZ-PT; Olympus, Macquarie Park, Australia). Images were captured at 1 frame per second for 30 seconds at 0.5 Hz using NIH ImageJ software. Swelling rates were determined from slope values of linear regression fits of relative volume as a function of time using Prism (GraphPad Software Inc., San Diego, CA, USA). Experiments were performed once, with seven to eight replicates.

Electrophysiological Recordings

Two-electrode voltage clamping was performed at room temperature in standard isotonic Na⁺ saline using a GeneClamp amplifier and pClamp 11 software (Molecular Devices, Sunnyvale, CA) as per published methods.⁴² Briefly, capillary glass pipettes (~1 MΩ) were filled with 1M KCl. From a holding potential of -40 mV, voltage steps from -120 to +60 mV were applied to measure conductance following stimulation with nitric oxide donor sodium nitroprusside (SNP; 200 μM) and extracellular applications of Cltx (1 μM). To investigate pharmacological inhibition by Cltx, after recording the initial response to SNP, oocytes were exposed to Cltx for 2 min. Additionally, selected oocytes ($n = 3$) were incubated with Cltx for 20 min prior to SNP application. Experiments were performed once, with at least three replicates.

Statistical Tests

Statistical analyses were performed with Prism using one-way ANOVA and appropriate *post-hoc* tests. Statistically significant results were represented as **** $p < 0.0001$, *** $p < 0.001$, ** $p < 0.01$, * $p < 0.05$, and ns (not significant) unless indicated otherwise. All data are shown as mean ± standard deviation. n -values are bracketed above x-axes. Boxplot histograms show 50% of data (boxes), the full range of data (error bars), and median values (central horizontal bars). Maroon data show effects of DMSO-soluble AqB011, cyanquixaline, verapamil and bicuculline standardised to vehicle controls. Blue data show effects of water-soluble Cltx, 4-aminopyridine and quisqualic acid standardised to untreated controls.

Results

Cltx significantly perturbed glioblastoma cell invasion but not migration

Effects of Cltx on three-dimensional invasion were assessed using transwell chamber assays with ECM-coated filters. In response to an FBS chemoattractant gradient, the invasiveness of U-87MG and U-251MG was measured in untreated and vehicle controls, and Cltx and AqB011 treatment conditions. Cells on undersides of filters (**Figure 2A**) were counted to determine percentages of invasion under the different treatment conditions. Compared to the untreated control, significantly decreased percentages of invasion were observed in response to 1 μM Cltx ($p < 0.01$) but not to 0.1 μM Cltx (**Figure 2B**).

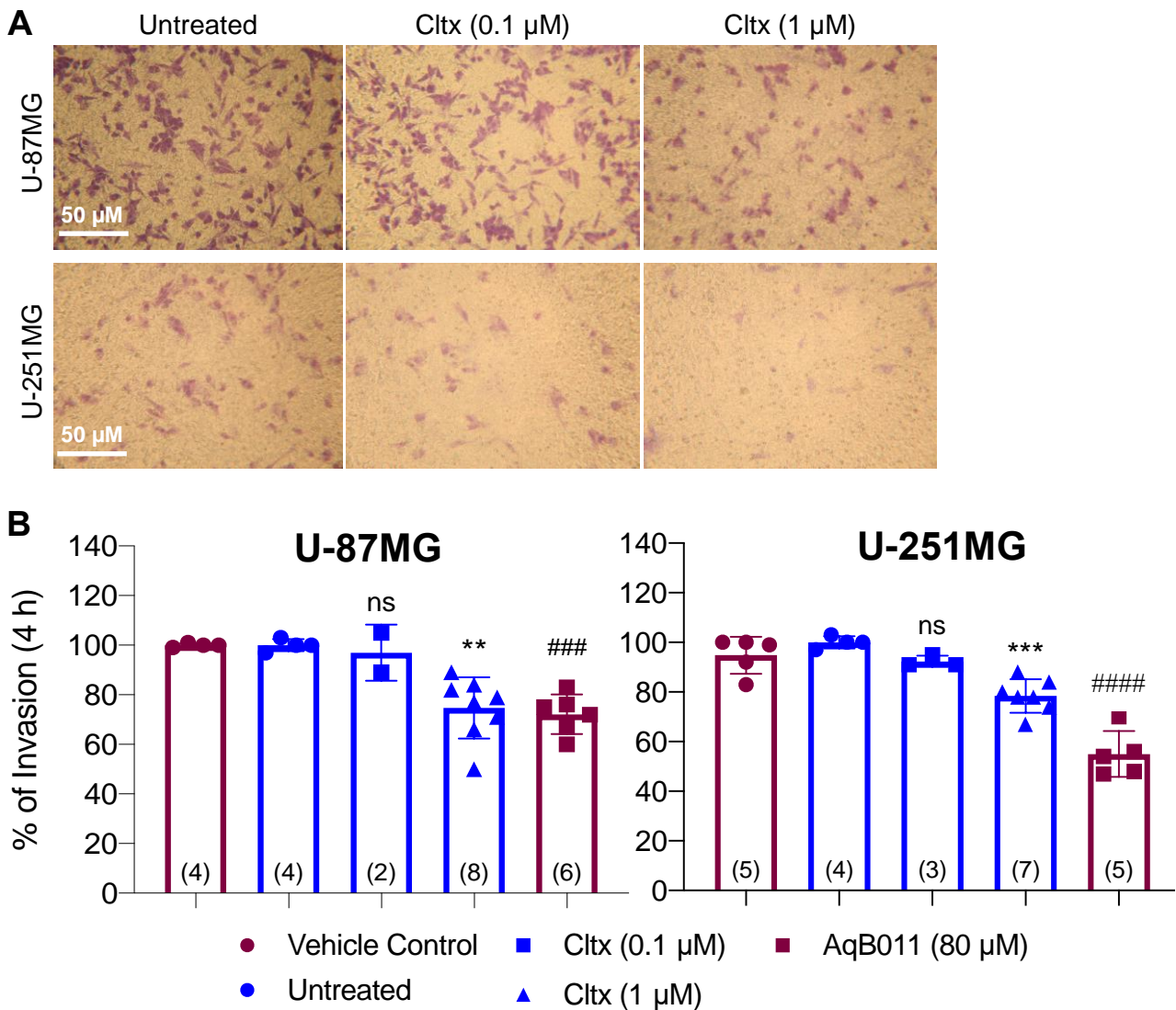


Figure 2: Effects of Cltx on cellular invasion in glioblastoma cell lines. **(A)** Cells stained on undersides of transwell membranes after traversing the filter. **(B)** Compiled data shown in histograms with invasion appropriately standardised as a percentage to mean values of vehicle or untreated controls. Statistical significance was determined with one-way ANOVA and Dunnett's *post-hoc* tests. *** $p < 0.001$, ** $p < 0.01$ and ns indicate statistical significance relative to untreated controls. ##### $p < 0.0001$ and ### $p < 0.001$ indicate significant differences from vehicle controls.

Wound closure assays assessed the effects of Cltx on two-dimensional cellular migration in U-87MG and U-251MG cells. Migration was calculated as a function of percent wound closure after 24 h based on initial wound areas at 0 h (**Figure 3A**). No significant inhibition of migration was observed in either cell line following treatment with 1 μM Cltx, as evidenced by similar percentages of wound closure calculated for Cltx-treated and untreated groups (**Figure 3B**).

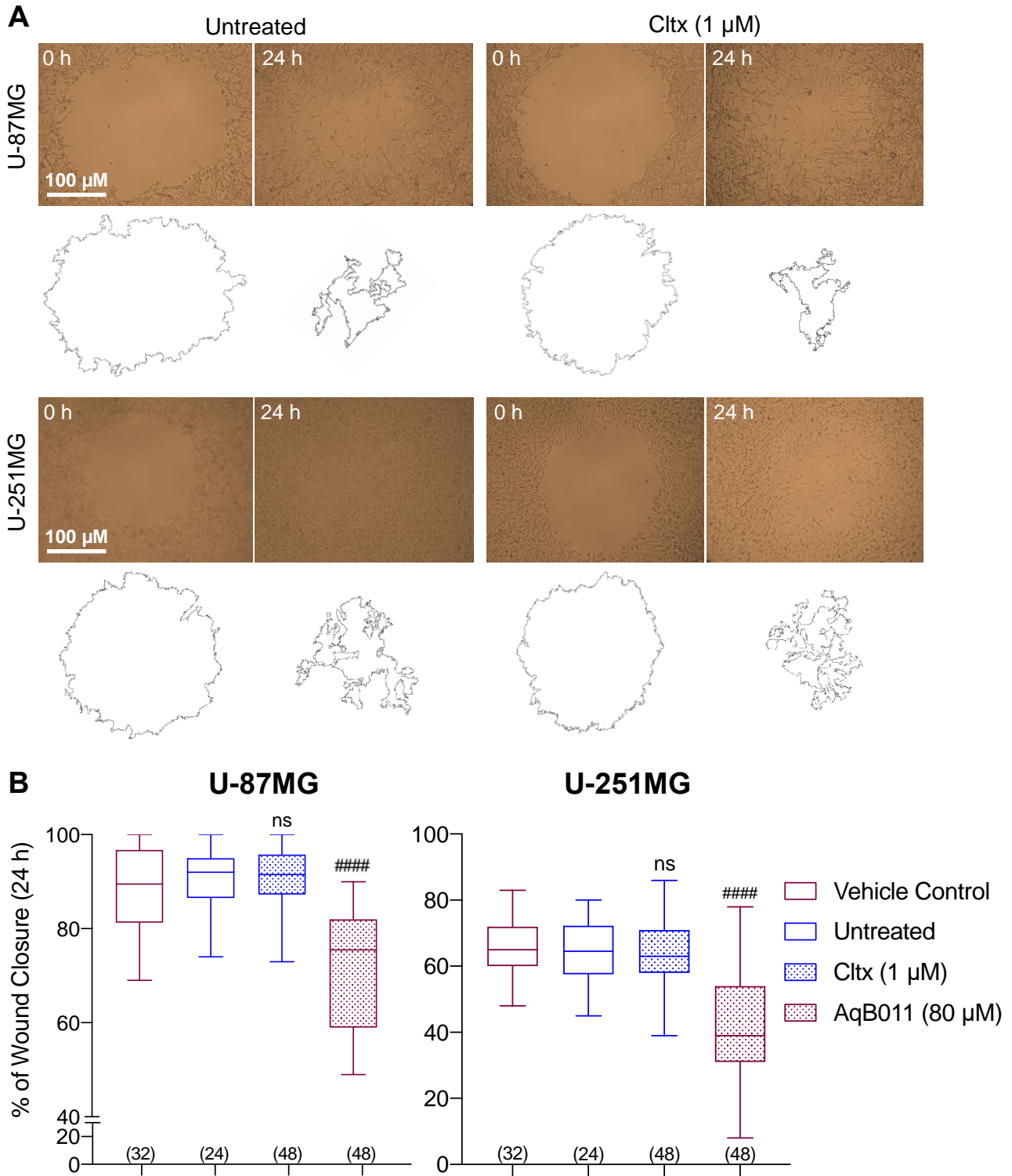


Figure 3: Effects of Cltx on cell migration in glioblastoma cell lines. **(A)** Wound areas imaged at 0 h and 24 h post-treatment with corresponding digital representations of wounds below (ImageJ). **(B)** Boxplot summary of wound closure in control and treatment groups quantified as the percentage of cell-occluded area 24 h post-wounding. Statistical significance was evaluated with one-way ANOVA and Dunnett’s *post-hoc* tests. ####*p* < 0.0001 and ns indicate statistical significance relative to vehicle and untreated controls respectively.

Cltx yielded no significant effects on AQP1 water or ion channel activity in *Xenopus laevis* oocytes

Effects of Cltx on AQP1 water and ion channel activity were determined using double swelling assays and two-electrode voltage clamp respectively. In 50% hypotonic saline, similarity between swelling rates of oocytes pre-incubated in isotonic saline \pm 1 μ M Cltx ($S2_{\pm Cltx}$) was indicated by the lack of significantly different swelling rates between $S2_{\pm Cltx}$ and S1 control oocytes seen in **Figure 4**.

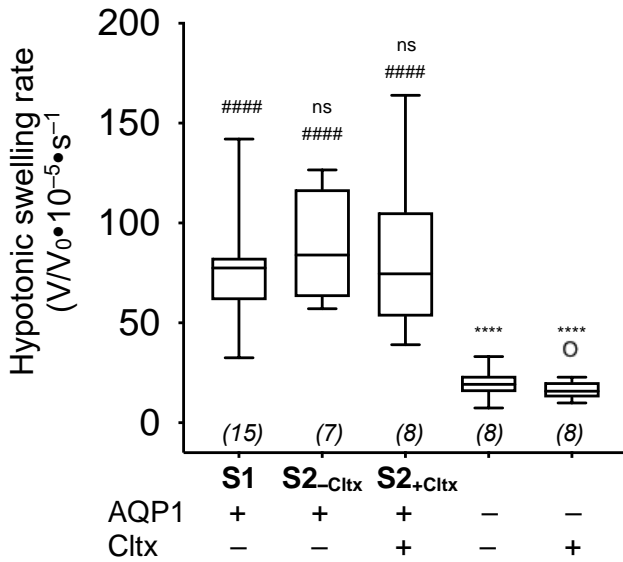


Figure 4: Lacking effects of Cltx on osmotic water permeability of oocytes. Boxplot data show oocyte swelling rates in 50% hypotonic saline \pm AQP1 and \pm Cltx. Swelling rates were calculated as ratios of final to initial oocyte volume as a function of time (s^{-1}). Statistical significance was determined with one-way ANOVA and Dunnett’s *post-hoc* tests. Significant differences from S1 control are indicated as **** $p < 0.0001$ and ns. Significant differences from AQP1⁻/Cltx⁻ control are indicated as ##### $p < 0.0001$ and O; not significant.

Two-electrode voltage clamp recordings of AQP1-expressing oocytes illustrated a lack of inhibition of AQP1 ion channel activity in response to Cltx. Negligible amplitude changes were observed when Cltx was applied acutely to SNP-activated ion channels (**Figure 5A**) whilst SNP activation still occurred following incubation of oocytes in Cltx for 20 min (**Figure 5B**). Current-voltage relationships derived from electrophysiological recordings (**Figure 5C**) and ionic conductance calculated at voltage steps between -120 and $+60$ mV compiled from at least three replicates illustrated that SNP stimulation was the only source of statistically significant difference ($p < 0.05$) in ionic conductance (**Figure 5D**).

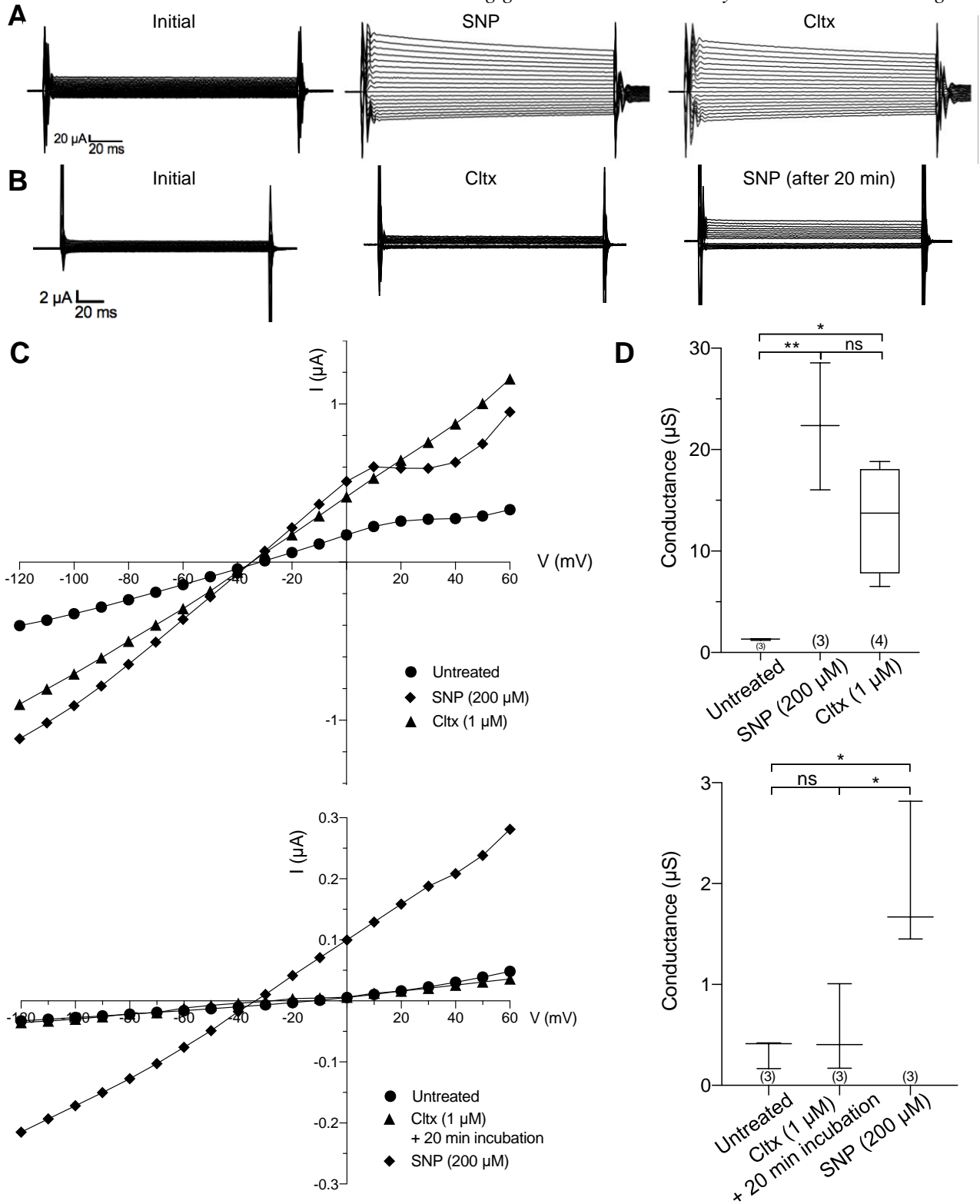


Figure 5: Effects of Cltx on AQP1-mediated ionic conductance in oocytes. **(A)** Two-electrode voltage clamp currents recorded before (initial) and after application of SNP and Cltx. **(B)** Currents recorded before and after 20 min incubation with Cltx followed by SNP stimulation. **(C)** Current-voltage relationships for traces shown in **(A)**; top and **(B)**; bottom, each averaged with two additional replicates. **(D)** Boxplot histograms of ionic conductance responses derived from slopes of current-voltage curves. Statistical significance is indicated as ** $p < 0.01$, * $p < 0.05$ and ns (one-way ANOVA with *post-hoc* Bonferroni tests).

Antagonists of AMPA/kainate, Ca_v and K_v channels significantly impaired glioblastoma cell invasion

Transwell chamber assays were also used to analyse the effects of cyanquixaline, verapamil, 4-aminopyridine, bicuculline and quisqualic acid on three-dimensional cellular invasion. Counting successfully invaded glioblastoma cells following exposure to these pharmacological agents (**Figure 6A**) revealed that in both cell lines, AMPA/kainate receptor antagonist cyanquixaline and Ca_v channel inhibitor verapamil significantly inhibited invasion ($p < 0.0001$), with invasion percentages comparable to that of AqB011 (**Figure 6B**). K_v channel inhibitor 4-aminopyridine curtailed invasion more significantly in U-251MG ($p < 0.0001$) than U-87MG ($p < 0.001$). GABA antagonist bicuculline and AMPA/kainate receptor agonist quisqualic acid elicited no significant inhibition of invasion in either cell line.

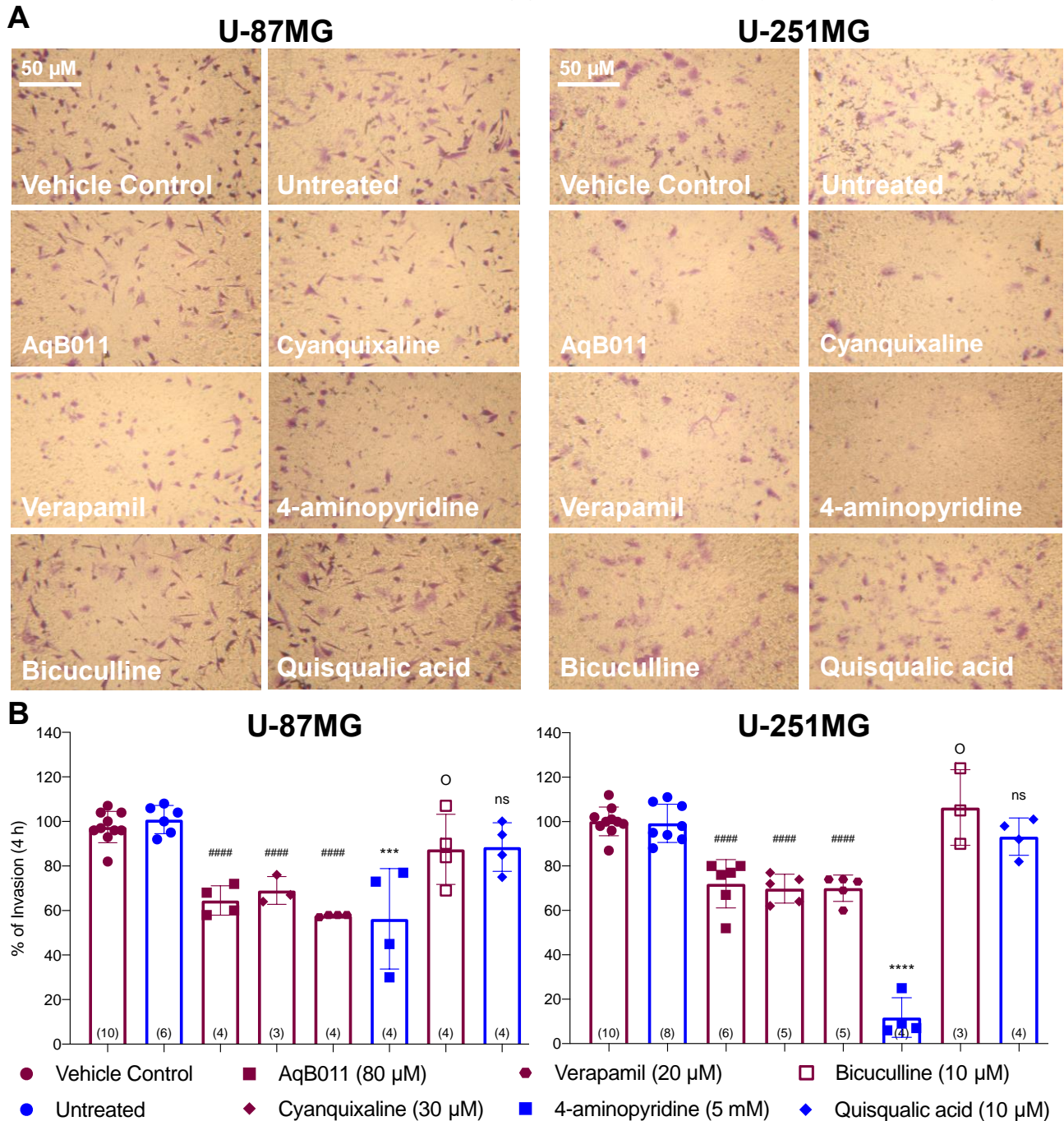


Figure 6: Effects of the tested modulators of glioblastoma-enriched targets on invasion in glioblastoma cell lines. **(A)** Stained cells that successfully traversed transwell filters in the presence of the compounds at concentrations indicated in the figure key. **(B)** Compiled data shown in histograms with invasion appropriately standardised as a percentage to the mean value of the vehicle or untreated control. Statistical significance was determined with one-way ANOVA and Dunnett's *post-hoc* tests. Significant differences from untreated controls are indicated by **** $p < 0.0001$, *** $p < 0.001$ and ns. Significant differences from vehicle controls are indicated by #### $p < 0.0001$ and O; not significant.

None of the tested compounds induced significant cytotoxicity at the highest concentrations used, as assessed by Alamar Blue assays (**Figure 7**). Impairment of cellular invasion observed following treatment with the antagonistic agents (including Cltx) was therefore not indirectly due to significantly reduced cell viability.

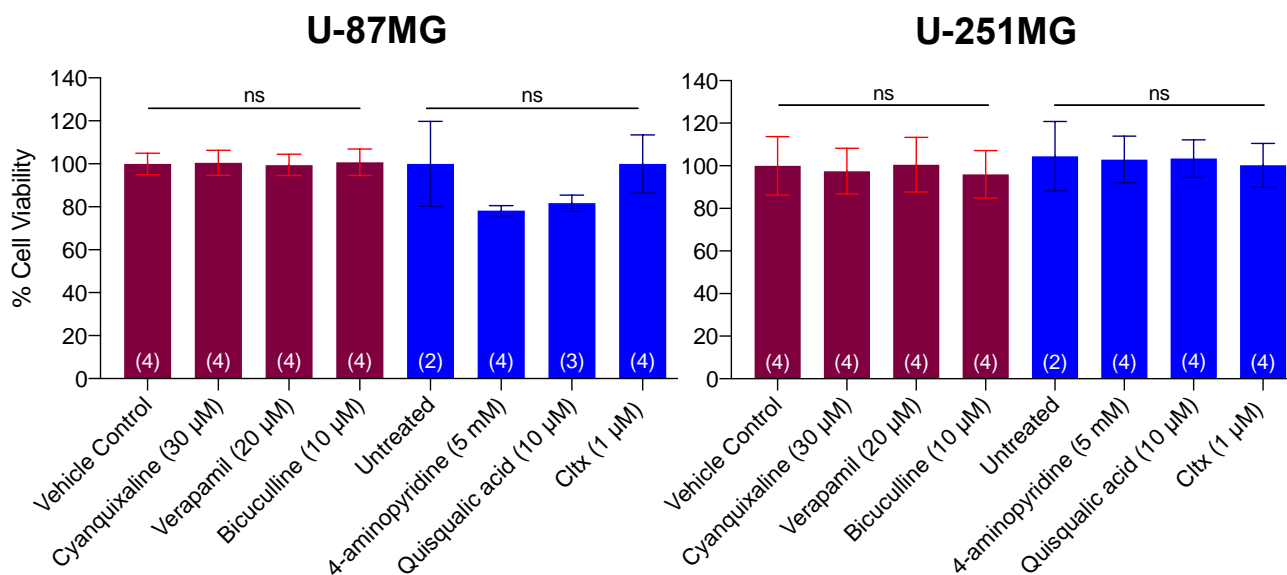


Figure 7: Effects of the tested compounds on U-87MG and U-251MG cell viability. Compiled data are shown in histograms with cell viability responses appropriately standardised as percentages to the mean values of vehicle or untreated controls. One-way ANOVA with Dunnett's *post-hoc* tests determined no significant differences between treatment groups and vehicle or untreated controls.

Discussion

Therapeutic strategies available to glioblastoma patients offer modest albeit measureable improvement to survival prospects. Radiotherapy and chemotherapy focus on abolishing rapidly dividing cells without necessarily eliminating risks of secondary neoplasms. Non-toxic inhibitors of cellular invasion that reduce glioblastoma motility within brain tissue are in high demand as adjuncts to these primary cancer therapies.

This project explored the existence of a novel interaction between AQP1 and Cltx that perturbs invasion and migration pathways in glioblastoma. Decreased cellular invasion observed upon Cltx exposure in U-87MG and U-251MG (**Figure 2B**) was consistent with previously reported decreased invasion in D-54MG and

CCF-STTG-1 cell lines following interaction of Cltx ($\leq 1 \mu\text{M}$) with metalloproteinase-2.¹⁷ This established interaction might underlie the glioblastoma cell invasion observed here, with results of wound closure assays suggesting a lack of effect of Cltx on AQP1 ion channels. Cltx did not impede two-dimensional wound closure in U-87MG or U-251MG at $1 \mu\text{M}$ (**Figure 3B**) to the same extent as AqB011, rendering AQP1, with established roles in both cellular invasion and migration,^{13,19} an unlikely target of Cltx.

Results of oocyte experiments also indicated that AQP1 does not present a novel target of Cltx. AQP1-expressing oocytes demonstrated similar swelling rates with and without Cltx exposure (**Figure 4**), indicating that Cltx had no significant effect on AQP1 water channels. Despite documentation of AQP1-mediated water movement facilitating glioma cell motility,^{13,19} results of these swelling assays do not contradict the Cltx-mediated inhibition of invasion observed in the transwell invasion assays (**Figure 2B**). AqB011 potently inhibiting glioblastoma cell invasion without affecting AQP1-mediated water transport¹⁵ is one demonstration of the independence with which AQP1 ion and water channels function. Additionally, Cltx did not significantly inhibit or prevent SNP-activated ionic conductance in AQP1-expressing oocytes (**Figure 5D**), further indicating the lack of interaction between Cltx and AQP1 ion channels. Incubating oocytes in Cltx for 20 min did not affect swelling rates in hypotonic saline or prevent stimulation of AQP1 ion channels with SNP, despite previous observations of Cltx eliciting its effects after approximately 20 min of exposure.¹⁴

Antagonists of AMPA/kainate, Ca_v and K_v channels (**Table 2**) inhibited invasion to varying extents in U-87MG and U-251MG at non-cytotoxic concentrations. Classification of U-87MG as mesenchymal⁴³ and U-251MG as proneural⁴⁴ indicates differences in gene and protein expression profiles and hence responses to pharmacological agents. These differences could underlie the diverse extents to which the antagonistic agents inhibited GBM cell invasiveness in U-87MG and U-251MG. However, this can only be conjectured on the basis of the transcriptomic information collected on the genes of interest from biopsied samples (**Figure 1**) and under the assumption that the resulting proteins localised to membranes of cultured cells to function correctly.

In various glioblastoma cell lines, Ca²⁺ signalling via Ca²⁺-permeable AMPA/kainate receptors has proven important to the cellular elongation processes that result in fusiform morphologies facilitative of invasiveness.^{23,45} Perturbation of such pathways could extend to U87-MG and U251-MG and underlie cyanquinoxaline-mediated inhibition of invasion (**Figure 6B**). Reduced invasion in U-87MG upon exposure to AMPA/kainate receptor agonist quisqualic acid is attributable to excitotoxicity (**Figure 7**), with quisqualic acid being one of the most potent AMPA agonists known.⁴⁶ Lack of significant inhibition of invasion by GABA_A receptor antagonist bicuculline reflects the low expression levels of GABRA1 by comparison to AMPA/kainate receptors seen in glioblastoma patient data (**Figure 1**; raw data available on the GBM Bio Discovery Portal).

Reduced U87-MG and U251-MG invasiveness following exposure to verapamil (**Figure 6B**) could have resulted from inhibition of Ca²⁺ flux via low voltage-activated Cav3 channels, a downstream effect of Cav3 channel blocker nifedipine that previously impaired *in vitro* glioblastoma cell proliferation.⁴⁷ However, with Ca²⁺ signalling involved in many cellular regulatory pathways,²⁴ inhibition of Cav channels with verapamil likely perturbs multiple downstream signalling cascades that facilitate glioblastoma motility in addition to proliferation, resulting in the verapamil-mediated impairment of invasion observed here.

Whilst cell cycle arrest following K_V channel inhibition is well established,^{29,30} the anti-invasive mechanisms of K_V channel inhibitor 4-aminopyridine are yet to be documented. Based on previous studies implicating K⁺ efflux in the cellular shrinkage processes facilitative of glioblastoma invasion,¹⁴ the significant impediment of glioblastoma cell invasion by 4-aminopyridine seen herein (**Figure 6B**) could be attributable to inhibition of K⁺ efflux via K_V channels.

In summary, the results herein reject the hypothesis that Cltx inhibits glioblastoma motility through a novel interaction with AQP1 ion channels. Results of transwell invasion and wound closure assays employed here showed that Cltx achieved significant inhibition of cellular invasion but not migration in U-87MG and U-251MG glioblastoma cell lines. Oocyte swelling assays and two-electrode voltage clamping showed that neither AQP1 water or ion channels were sensitive to 1 μM Cltx. Although effects of greater Cltx concentrations on cellular migration in U-87MG and U-251MG cells, and on AQP1-mediated oocyte

swelling rates and ionic conductance were not investigated on this occasion, the plausibility of AQP1 being an alternate target of Cltx is still unlikely given (1) the cellular responses evoked at lower Cltx concentrations upon interaction with known targets^{17,18} and (2) failure to inhibit *in vitro* glioblastoma migration to the same extent as AQP1 ion channel antagonist AqB011.⁴⁸ Cyanquixaline, verapamil and 4-aminopyridine significantly impaired cellular invasion in U-87MG and U-251MG at non-cytotoxic concentrations and to varying extents following perturbation of signalling pathways downstream of AMPA/kainate, Cav and Kv channels.

Elucidating the (1) lowest concentrations of these agents that elicit significantly potent inhibition of glioblastoma invasion and (2) off-target effects arising from widespread expression of AMPA/kainate, Cav and Kv channels in complex *in vivo* systems present a challenge going forward. Additionally, with survival plots for the gene clusters in **Figure 1** showing stronger PIHRs than that of any gene alone (**Table 1**), combining pharmacological agents that modulate multiple glioblastoma-enriched signalling proteins implicated in key motility pathways could prove more effective in realising clinically relevant inhibition of glioblastoma invasiveness. Defining an optimised combination of agents that acts synergistically to halt glioblastoma invasion without cytotoxic side-effects could initiate a novel way of limiting glioblastoma motility during administration of primary clinical treatments. On a broader scale, tailoring pharmacological interventions to the genetic make-ups of different of tumour types could significantly advance large-scale management of tumour invasiveness.

Words: 4,500

Acknowledgements

Funding support for this research was provided by the Australian Research Council (grant DP190101745) and the Jemima Lendrum Honours Grant for Cancer Research. I wish to thank Professor Mehdi Mobli from the University of Queensland for providing the chlorotoxin and the Aquaporin Physiology and Drug Discovery Research Team for the invaluable assistance provided on this project. I pay special regards to Saeed Nourmohammadi for laboratory training and support and express the highest gratitude to my supervisor, Professor Andrea Yool, who offered guidance and advice throughout every aspect of this project.

References

1. Packer RJ, MacDonald T & Vezina G (2008). Central Nervous System Tumors. *Pediatr Clin North Am* **55**, 121-45.
2. Chakravarti A, Chakladar A, Delaney MA, Latham DE & Loeffler JS (2002). The Epidermal Growth Factor Receptor Pathway Mediates Resistance to Sequential Administration of Radiation and Chemotherapy in Primary Human Glioblastoma Cells in a RAS-dependent Manner. *Cancer Res* **62**, 4307-15.
3. Stupp R, Mason WP, van den Bent MJ, Weller M, Fisher B, Taphoorn MJ, Belanger K, Brandes AA, Marosi C, Bogdahn U, Curschmann J, Janzer RC, Ludwin SK, Gorlia T, Allgeier A, Lacombe D, Cairncross JG, Eisenhauer E & Mirimanoff RO (2005). Radiotherapy plus concomitant and adjuvant temozolomide for glioblastoma. *N Engl J Med* **352**, 987-96.
4. Gashaw I, Ellinghaus P, Sommer A & Asadullah K (2011). What makes a good drug target? *Drug Discovery Today* **16**, 1037-43.
5. Holford NHG & Atkinson AJ (2012). Chapter 21 - Time Course of Drug Response. In *Principles of Clinical Pharmacology (Third Edition)*, edn, ed. Atkinson AJ, Huang S-M, Lertora JLL & Markey SP, 357-67. Academic Press.
6. Verhaak RG, Hoadley KA, Purdom E, Wang V, Qi Y, Wilkerson MD, Miller CR, Ding L, Golub T, Mesirov JP, Alexe G, Lawrence M, O'Kelly M, Tamayo P, Weir BA, Gabriel S, Winckler W, Gupta S, Jakkula L, Feiler HS, Hodgson JG, James CD, Sarkaria JN, Brennan C, Kahn A, Spellman PT, Wilson RK, Speed TP, Gray JW, Meyerson M, Getz G, Perou CM & Hayes DN (2010). Integrated genomic analysis identifies clinically relevant subtypes of glioblastoma characterized by abnormalities in PDGFRA, IDH1, EGFR, and NF1. *Cancer Cell* **17**, 98-110.
7. Yool AJ & Ramesh S (2020). Molecular Targets for Combined Therapeutic Strategies to Limit Glioblastoma Cell Migration and Invasion. *Front Pharmacol* DOI: 10.3389/fphar.2020.00358.
8. Zeidel ML, Ambudkar SV, Smith BL & Agre P (1992). Reconstitution of Functional Water Channels in Liposomes Containing Purified Red Cell CHIP28 Protein. *Biochemistry* **31**, 7436-40.
9. Finn RN & Cerdà J (2015). Evolution and functional diversity of aquaporins. *Biol Bull* **229**, 6-23.
10. Anthony TL, Brooks HL, Boassa D, Leonov S, Yanochko GM, Regan JW & Yool AJ (2000). Cloned Human Aquaporin-1 Is a Cyclic GMP-Gated Ion Channel. *Mol Pharmacol* **57**, 576-88.

11. Pei JV, Heng S, De Ieso ML, Sylvia G, Kourghi M, Nourmohammadi S, Abell AD & Yool AJ (2019). Development of a Photoswitchable Lithium-Sensitive Probe to Analyze Nonselective Cation Channel Activity in Migrating Cancer Cells. *Mol Pharmacol* **95**, 573-83.
12. Takata K, Matsuzaki T & Tajika Y (2004). Aquaporins: water channel proteins of the cell membrane. *Prog Histochem Cytochem* **39**, 1-83.
13. Yang WY, Tan ZF, Dong DW, Ding Y, Meng H, Zhao Y, Xin XF & Bi W (2018). Association of aquaporin1 with tumor migration, invasion and vasculogenic mimicry in glioblastoma multiforme. *Mol Med Rep* **17**, 3206-11.
14. McFerrin MB & Sontheimer H (2006). A role for ion channels in glioma cell invasion. *Neuron Glia Biol* **2**, 39-49.
15. De Ieso ML, Pei JV, Nourmohammadi S, Smith E, Chow PH, Kourghi M, Hardingham JE & Yool AJ (2019). Combined pharmacological administration of AQP1 ion channel blocker AqB011 and water channel blocker Bacopaside II amplifies inhibition of colon cancer cell migration. *Sci Rep* **9**, 12635-50.
16. DeBin JA, Maggio JE & Strichartz GR (1993). Purification and characterization of chlorotoxin, a chloride channel ligand from the venom of the scorpion. *Am J Physiol: Cell Physiol* **264**, 361-9.
17. Deshane J, Garner CC & Sontheimer H (2003). Chlorotoxin inhibits glioma cell invasion via matrix metalloproteinase-2. *J Biol Chem* **278**, 4135-44.
18. Kesavan K, Ratliff J, Johnson EW, Dahlberg W, Asara JM, Misra P, Frangioni JV & Jacoby DB (2010). Annexin A2 Is a Molecular Target for TM601, a Peptide with Tumor-targeting and Anti-angiogenic Effects. *J Biol Chem* **285**, 4366-74.
19. Saadoun S, Papadopoulos MC, Hara-Chikuma M & Verkman AS (2005). Impairment of angiogenesis and cell migration by targeted aquaporin-1 gene disruption. *Nature* **434**, 786-92.
20. Reiner A & Levitz J (2018). Glutamatergic Signaling in the Central Nervous System: Ionotropic and Metabotropic Receptors in Concert. *Neuron* **98**, 1080-98.
21. Traynelis SF, Wollmuth LP, McBain CJ, Menniti FS, Vance KM, Ogden KK, Hansen KB, Yuan H, Myers SJ & Dingledine R (2010). Glutamate receptor ion channels: structure, regulation, and function. *Pharmacol Rev* **62**, 405-96.

22. Ishiuchi S, Yoshida Y, Sugawara K, Aihara M, Ohtani T, Watanabe T, Saito N, Tsuzuki K, Okado H, Miwa A, Nakazato Y & Ozawa S (2007). Ca²⁺-permeable AMPA receptors regulate growth of human glioblastoma via Akt activation. *J Neurosci* **27**, 7987-8001.
23. Ishiuchi S, Tsuzuki K, Yoshida Y, Yamada N, Hagimura N, Okado H, Miwa A, Kurihara H, Nakazato Y, Tamura M, Sasaki T & Ozawa S (2002). Blockage of Ca²⁺-permeable AMPA receptors suppresses migration and induces apoptosis in human glioblastoma cells. *Nat Med* **8**, 971-8.
24. Tsien RW, Hess P, McCleskey EW & Rosenberg RL (1987). Calcium channels: mechanisms of selectivity, permeation, and block. *Annu Rev Biophys Biophys Chem* **16**, 265-90.
25. Perez-Reyes E & Schneider T (1994). Calcium channels: Structure, function, and classification. *Drug Dev Res* **33**, 295-318.
26. Panner A, Cribbs LL, Zainelli GM, Origitano TC, Singh S & Wurster RD (2005). Variation of T-type calcium channel protein expression affects cell division of cultured tumor cells. *Cell Calcium* **37**, 105-19.
27. Gutman GA, Chandy KG, Grissmer S, Lazdunski M, Mckinnon D, Pardo LA, Robertson GA, Rudy B, Sanguinetti MC & Stühmer W (2005). International Union of Pharmacology. LIII. Nomenclature and molecular relationships of voltage-gated potassium channels. *Pharmacol Rev* **57**, 473-508.
28. Zhai J, Lin QS, Hu Z, Wong R & Soong TW (2016). Alternative Splicing and RNA Editing of Voltage-Gated Ion Channels: Implications in Health and Disease. In *Ion Channels in Health and Disease*, 1st edn, ed. Pitt GS, 265-92. Academic Press, Cambridge.
29. Shah NH & Aizenman E (2014). Voltage-gated potassium channels at the crossroads of neuronal function, ischemic tolerance, and neurodegeneration. *Transl Stroke Res* **5**, 38-58.
30. Chittajallu R, Chen Y, Wang H, Yuan X, Ghiani CA, Heckman T, McBain CJ & Gallo V (2002). Regulation of Kv1 subunit expression in oligodendrocyte progenitor cells and their role in G1/S phase progression of the cell cycle. *Proc Natl Acad Sci U S A* **99**, 2350-5.
31. Lin YM, Jan HJ, Lee CC, Tao HY, Shih YL, Wei HW & Lee HM (2008). Dexamethasone reduced invasiveness of human malignant glioblastoma cells through a MAPK phosphatase-1 (MKP-1) dependent mechanism. *Eur J Pharmacol* **593**, 1-9.

32. Piette C, Deprez M, Roger T, Noël A, Foidart JM & Munaut C (2009). The dexamethasone-induced inhibition of proliferation, migration, and invasion in glioma cell lines is antagonized by macrophage migration inhibitory factor (MIF) and can be enhanced by specific MIF inhibitors. *J Biol Chem* **284**, 32483-92.
33. Guan Y, Chen J, Zhan Y & Lu H (2018). Effects of dexamethasone on C6 cell proliferation, migration and invasion through the upregulation of AQP1. *Oncol Lett* **15**, 7595-7602.
34. Ye ZC & Sontheimer H (1999). Glioma cells release excitotoxic concentrations of glutamate. *Cancer Res* **59**, 4383-91.
35. Bowles AP, Pantazis CG & Wansley W (1990). Use of verapamil to enhance the antiproliferative activity of BCNU in human glioma cells: an in vitro and in vivo study. *J Neurosurg* **73**, 248-253.
36. Ru Q, Li WL, Xiong Q, Chen L, Tian X & Li CY (2018). Voltage-gated potassium channel blocker 4-aminopyridine induces glioma cell apoptosis by reducing expression of microRNA-10b-5p. *Mol Biol Cell* **29**, 1125-36.
37. Birkle DL & Wiley KS (1991). Bicuculline induces free fatty acid release from phospholipids in Neuro-2A cells in culture. *Neurochem Res* **16**, 1285-93.
38. Zhang C, Yuan XR, Li HY, Zhao ZJ, Liao YW, Wang XY, Su J, Sang SS & Liu Q (2015). Anti-cancer effect of metabotropic glutamate receptor 1 inhibition in human glioma U87 cells: involvement of PI3K/Akt/mTOR pathway. *Cell Physiol Biochem* **35**, 419-32.
39. Justus CR, Leffler N, Ruiz-Echevarria M & Yang LV (2014). In vitro cell migration and invasion assays. *J Vis Exp* **88**, e51046.
40. O'Brien J, Wilson I, Orton T & Pognan F (2000). Investigation of the Alamar Blue (resazurin) fluorescent dye for the assessment of mammalian cell cytotoxicity. *Eur J Biochem* **267**, 5421-6.
41. Kourghi M, De Ieso ML, Nourmohammadi S, Pei JV & Yool AJ (2018). Identification of Loop D Domain Amino Acids in the Human Aquaporin-1 Channel Involved in Activation of the Ionic Conductance and Inhibition by AqB011. *FRONT CHEM* **6**, 142-53.
42. Boassa D & Yool AJ (2003). Single amino acids in the carboxyl terminal domain of aquaporin-1 contribute to cGMP-dependent ion channel activation. *BMC Physiol* **3**, 12.
43. Breznik B, Motaln H, Vittori M, Rotter A & Lah Turnšek T (2017). Mesenchymal stem cells differentially affect the invasion of distinct glioblastoma cell lines. *Oncotarget* **8**, 25482-99.

44. Zhao K, Cui X, Wang Q, Fang C, Tan Y, Wang Y, Yi K, Yang C, You H, Shang R, Wang J & Kang C (2019). RUNX1 contributes to the mesenchymal subtype of glioblastoma in a TGF β pathway-dependent manner. *Cell Death Dis* **10**, 877.
45. Ribeiro MP, Custodio JB & Santos AE (2017). Ionotropic glutamate receptor antagonists and cancer therapy: time to think out of the box? *Cancer Chemother Pharmacol* **79**, 219-25.
46. Jin R, Horning M, Mayer ML & Gouaux E (2002). Mechanism of Activation and Selectivity in a Ligand-Gated Ion Channel: Structural and Functional Studies of GluR2 and Quisqualate. *Biochemistry* **41**, 15635-43.
47. Zhang Y, Zhang J, Jiang D, Zhang D, Qian Z, Liu C & Tao J (2012). Inhibition of T-type Ca²⁺ channels by endostatin attenuates human glioblastoma cell proliferation and migration. *Br J Pharmacol* **166**, 1247-60.
48. Kourghi M, Pei JV, De Ieso ML, Flynn G & Yool AJ (2016). Bumetanide Derivatives AqB007 and AqB011 Selectively Block the Aquaporin-1 Ion Channel Conductance and Slow Cancer Cell Migration. *Mol Pharmacol* **89**, 133-40.